Hybrid vesicles from lipids and block copolymers: phase behavior from the micro- to the nano-scale

C. Magnani[1,2], C. Montis[2], G. Mangiapia[3], A-F Mingotaud[1], C. Mingotaud[1], C. Roux[1], P. Joseph[4], D. Berti[1], B. Lonetti[1,]*

[1] Université de Toulouse; UPS/CNRS UMR 5623; IMRCP, 118 route de Narbonne, F-31062, Toulouse Cedex 9, France.
[2] Department of Chemistry, University of Florence and CSGI, via della Lastruccia 3, 50019, Florence (Italy)
[3] Forschungszentrum Jülich GmbH; Jülich Centre for Neutron Science. Außenstelle am Heinz Maier-Leibnitz Zentrum, Lichtenbergstraße 1, D-85747 Garching, Germany.
[4] LAAS-CNRS, Université de Toulouse, CNRS, Toulouse, France

HIGHLIGHTS

- Phospholipid (DPPC)-copolymer (PBD-PEO) hybrid assemblies are investigated at different lengthscales
- Micron-sized hybrid assemblies are giant vesicles characterized by phase-segregated domains
- The domains strongly affect the morphological and viscoelastic properties of GUVs
- Nano-sized hybrids are preferentially arranged into worm-like shapes
- It is possible to tune the physicochemical-mechanical features of nano- and micro-hybrids

ABSTRACT

In recent years, there has been a growing interest in the formation of copolymers-lipids hybrid self-assemblies, which allow combining and improving the main features of pure lipids-based and copolymer-based systems known for their potential applications in the biomedical field. In

this contribution we investigate the self-assembly behavior of dipalmitoylphosphatidylcholine (DPPC) mixed with poly(butadiene-b-ethyleneoxide) (PBD-PEO), both at the micro- and at the nano-length scale.

Epifluorescence microscopy and Laser Scanning Confocal microscopy are employed to characterize the morphology of micron-sized hybrid vesicles and the presence of fluid-like inhomogeneities in their membrane has been evidenced in all the investigated range of compositions. Furthermore, a microfluidic set-up characterizes the mechanical properties of the prepared assemblies by measuring their deformation upon flow: hybrids with low lipid content behave like pure polymer vesicles, whereas objects mainly composed of lipids show more variability from one vesicle to the other. Finally, the structure of the nanosized assemblies is characterized through a combination of Dynamic Light Scattering, Small Angle Neutron Scattering and Transmission Electron Microscopy. A vesicles-to-wormlike transition has been evidenced due to the intimate mixing of DPPC and PBD-PEO at the nanoscale. Combining experimental results at the micron and at the nanoscale improves the fundamental understanding on the phase behavior of copolymer-lipid hybrid assemblies, which is a necessary prerequisite to tailor efficient copolymer-lipid hybrid devices.

KEYWORDS liposomes; polymersomes; GUVs; microfluidics; self-assembly; surfactant; polymer

1. INTRODUCTION

Since their first description by Disher and Eisenberg [1], polymersomes have raised the interest of the scientific community because of their mechanical stability and tunable chemical design. Their possible applications span from nanocarriers for drug delivery, medical imaging, advanced

nanoreactors or electronics to protocells mimicking cell structure and functions [2]. On the other hand, the structural membrane components, lipids, are biocompatible but their long-term stability is limited. Hybrid lipid/polymer vesicles combine the inherent advantages of their components: the biocompatibility of lipids and the mechanical stability and chemical versatility of copolymers. The research on this topic is still in its infancy, and most of it deals with giant vesicles [3] in the effort to understand their phase diagram, miscibility and stability limits, and tune their morphology and structural features within the bilayer. The few examples about hybrid nanovesicles [4–10] mainly deal with the assessment of their dual nature, possible applications to drug delivery and recently the existence of phase separation at the nanoscale. The parameters influencing their morphology and phase separation are far from being understood. Moreover, studies concerning hybrid systems leading both to nano-objects and giant vesicles are very scarce [6,9]. With respect to giant vesicles, polydimethylsiloxane (PDMS), polybutadiene (PBD) and polyisobutylene (PIB) are the most thoroughly investigated hydrophobic blocks, as they do not crystallize at room or body temperature and possess a glass transition temperature below 0°C, which guarantees a sufficient flexibility of the polymer chains during the commonly used electroformation process (*i.e.* electric field-assisted film hydration). The observed hybrid vesicles can be homogeneous or inhomogeneous with lateral domains. PDMS and PBD based block copolymers with different molecular weights have been studied in blends with lipids in the liquid (POPC, 2-Oleoyl-1-palmitoyl-sn-glycero-3-phosphocholine) and gel (DPPC, dipalmitoylphosphatidylcholine) phase. The effects of size mismatch of the hydrophobic blocks and lipid fluidity on giant vesicle homogeneity have started to be systematically investigated for PDMS based copolymers. In this case, it was demonstrated that the hydrophobic mismatch is an important parameter for lipids in the fluid phase. Indeed, when the block copolymer molecular

weight increases, homogeneous vesicles form in a larger range of compositions in the region of low lipid content [5,11]. At higher lipid content phase-separated vesicles form, and budding is observed; phase-separated vesicles are not stable and budding degenerates in vesicle fission for copolymers of higher molecular weights. In this case, a high percentage of pure lipid or polymer vesicles is always observed, resulting from fission phenomena. This also explains the experimental results on PBD based block copolymers in the case of high hydrophobic mismatch. In this case, homogeneous hybrid vesicles form in the polymer-rich domain; and in the lipid-rich domain homogeneous hybrid vesicles form together with vesicles of the pure components. POPC gives rise to homogeneous giant vesicles in a restricted range of compositions [12] for PBD based copolymers, while for PDMS based triblock copolymers, vesicles always form. On the other hand, DPPC always form inhomogeneous systems with domains independently of the hydrophobic mismatch in the case of PDMS copolymers [11]. Homogeneous GUVs (Giant Unilamellar Vesicles) are also observed for PIB block copolymers in the lipid-rich and polymer-rich regions (below 18 mol% and above 30 mol% DPPC), while phase separation occurs only for intermediate compositions [13]. For DPPC hybrid systems, electroformation is conducted above lipid melting temperature and phase separation occurs after cooling down to room temperature. The cooling rate affects domains size and shape, fast cooling producing round domains whereas slow cooling produces flower-like or irregular shape domain. For higher mismatches, round domains formed, irrespectively of the cooling rate. In the case of PIB and PDMS based block copolymers, hybrid vesicles form in all the range of composition, for PBD based copolymers only one composition has been reported. As mentioned above, small unilamellar vesicles were also investigated for a few systems, composed of lipids both in the gel and liquid phase. The vesicles' hydrodynamic radius [6–8] and permeability together with changes in the thermal

properties of the bilayer [7,8] are used as an indication of the hybrid nature of the vesicles. Hybrid vesicles are more stable than liposomes and the effect was related to literature results on the higher stability of pegylated liposomes [7]. Vesicles permeability always decreases in the presence of the block copolymers. On the other hand, the effect on the hydrodynamic size is difficult to rationalize due to the lack of systematic studies using copolymer with different molecular weight and above all it is not always in agreement with the effects on the bilayer properties. In the case of PDMS based triblock copolymers [7], for example, the copolymer with the highest mismatch induced the largest effect on permeability and melting temperature of hybrid DPPC-polymer vesicles, but less impact on the vesicles' size. Very recently Dao et al. [11] underlined the need for more detailed investigations on the morphology of the nanostructures, the distributions of the components in the bilayers in order to understand the important parameters (i.e. chemical nature, curvature and hydrophobic mismatch) involved. This could also shed some light on the correlation between behaviors at the micro and nano scales if it exists.

Here we report a study on vesicles, both at the micro- and nanoscales, formed by PBD_{43}-PEO_{20} and DPPC. Although PBD *per se* is not biodegradable, the conjugation with PEO makes PBD-PEO block copolymer biocompatible [14]. In addition, it is well established that PEO improves the pharmacokinetic properties of nanodrugs and drug delivery nanodevices, due a stealth effect hindering the recognition by the mononuclear phagocyte system (MPS) [15,16] Thus, PBD-PEO based systems have been recently proposed for biomedical applications as drug carriers, and investigated both *in vitro* and *in vivo* [17,18]. Concerning the lipid building block DPPC, though generally not present in biological membranes, is fully biocompatible and thus of general interest for biomedical applications. In particular, due to the fully saturated nature of the hydrophobic

chain, pure DPPC assemblies are characterized by a relatively high melting temperature (41°C, [19]), of particular relevance for the design and development of smart temperature responsive drug delivery systems [20]. We have established the phase diagram in all the range of compositions by microscopy techniques (epifluorescence and scanning confocal microscopy) in the case of GUV obtained by electroformation, and by scattering techniques in the case of nanovesicles obtained by film rehydration and extrusion.

2. MATERIALS AND METHODS

2.1 Materials

PBD-PEO (PBD(2300)PEO(900) □(polybutadiene (Mw 2300)-b-polyethyleneoxide (Mw 900))) was purchased from Polymer Source Inc. (Dorval Montréal, Canada) and characterized by ^{1}H NMR and Size Exclusion Chromatography. DPPC (dipalmitoylphosphatidylcholine) and β-Bodipy 2-(4,4-diuoro-5,7-dimethyl-4-bora-3a,4adiaza- sindacene- 3-pentanoyl)-1 hexadecanoyl-sn-glycero-3-phosphocholine were purchased from Avanti Polar Lipids, Inc. (Alabaster, AL). DiI-C20 (1,1′-dieicosanyl-3,3,3′,3′-tetramethylindocarbocyanine perchlorate) was purchased from Molecular Targeting Technologies (Westchester, PA), OG-DHPE (Oregon Green™ 488 1,2-Dihexadecanoyl-sn-Glycero-3-Phosphoethanolamine) was purchased from Invitrogen Life Technologies (Saint Aubin, France). D_2O, MeOH, $CHCl_3$, sucrose were provided by Sigma-Aldrich (St. Louis, MO).

2.2 Preparation of Giant Unilamellar Vesicles

Giant Unilamellar Vesicles (GUVs) were prepared on a *Vesicles prep pro* instrument produced by Nanion. It is based on the well-known electroformation method described for the first time by

Angelova et al. [21] for lipid-based GUVs. Briefly, 5 µl of a 1 mg/ml solution of the polymer in chloroform, lipid or their blend was deposited (approximately 1 cm^2) on an ITO-coated glass slide and dried under vacuum. Then an electroformation chamber was built-up by surrounding the dry film with a 1 mm o-ring and it was subsequently filled with 250 µl of a 240 mM sucrose solution. The chamber was closed with another ITO-coated glass slide and connected to an alternate current generator through electrodes connected with the ITO-coated glass slides. A peak-to-peak voltage of 3 volts and 10 Hz was then applied at 50 °C for one hour to form the GUVs. The temperature and the voltage were then slowly decreased and the vesicles were collected with a pipette.

2.3 Preparation of Small Unilamellar Vesicles

Nano-sized vesicles were prepared by the method of film rehydration. Briefly, 1 mg/mL solutions of pure lipid, pure polymer or lipid/polymer blend were prepared in chloroform. A dry film from 1 ml of solution was obtained in a glass tube by evaporating the solvent on a rotavapor for at least for 3 hours. Then, 1.5 ml of MilliQ water were added and the film was bath-sonicated at 50 °C for 15 minutes. The obtained dispersions were then extruded 11 times at 50 °C through a 100 nm-pore sized polycarbonate membrane. For SANS investigations the procedure adopted was similar except that D_2O was used instead of H_2O.

2.4 Optical Microscopy

Optical microscopy images were acquired on an Olympus Microscope 100W BX 53 using a 20x objective and then analysed with ImageJ.

2.5 Confocal Laser Scanning Microscopy

The fluorescent dyes β-Bodipy and DiI-C20 were excited respectively at 488 nm, with an Ar laser, and 561 nm, with DPSS 561 laser, and the fluorescence was collected with PMTs in the wavelength ranges 498-530 nm and 571-630 nm, respectively. It must be noted that in order to facilitate the formation of PBD-PEO GUVs of sufficient size and their detachment from the film, which is necessary for confocal microscopy visualization, for the preparation of pure copolymer-based vesicles, PBD-PEO was mixed with 20 mol % PBD-PEO-COOH.

2.6 Microfluidics

Microfluidic chips fabrication and design. Polydimethylsiloxane (PDMS) - glass microfluidic chips were fabricated using standard soft-lithography techniques [22]. The mold (50 µm thick) was prepared by lamination and photolithography of a dry film on a silicon wafer, as described in [23]. PDMS / crosslinking agent (Sylgard 184) 10:1 mixture was casted on the mold and cured for 1 hour and 30 min at 80°C. After unmolding, holes for fluid access were punched (biopsy punch, Ted Pella, 1mm diameter). Chip bonding was achieved by putting the PDMS in contact with a glass coverslip after exposing both surfaces to oxygen plasma for 30s. Chips were finally cured 10 min at 70°C to improve the sealing. The geometry (designed with Clewin software) consisted in 1 cm-long straight channels, with rectangular cross section (350 µm x 50 µm), including U-shaped structures distributed along the channel to trap the vesicles and measure their deformation. Lateral opening of the traps ranged from 10 to 20 µm.

Microfluidics experiments. In order not to inject too many vesicles, 50 µL of the solution obtained by electroformation was diluted to 1 mL with a 240 mM aqueous sucrose solution, filtered at 0.2 µm. The obtained solution was injected at a fixed pressure, ranging from 0.5 to 50 mBar, thanks to a fluid reservoir (Flowell, Fluigent) connected to a pressure controller (MFCS,

Fluigent) by standard tubing (1/16'' OD, 0.81mm ID). Chips were put at least 20 min under vacuum before the experiments to help eliminating possible bubbles trapped during filling. Prior to the injection of the solution containing the GUV, a 2% BSA (Bovine Serum Albumin) aqueous solution was flown within the chip for 10 min in order to avoid vesicle adhesion on channel's walls. Characterization was achieved by imaging, either by standard epifluorescence microscopy (Olympus IX70 microscope, 50x objective) connected to an EMCCD video camera (Andor Ixon), or by Confocal Laser Scanning Microscopy CLSM (Leica TCS SP2).

2.7 Dynamic Light Scattering and Multi-angle Dynamic Light Scattering

DLS measurements were performed with an instrument from Malvern (Orsay, France) Zetasizer NanoZS at an angle of 173°. The samples were measured after the preparation without dilution and at 25 °C. Multiangle dynamic light scattering was performed with a LS Spectrometer (LSinstruments) measuring the scattering from 15° to 150° each 5°. The curves were analysed with a home-made program [24]. The autocorrelation function has been fitted using the Non-Negatively constrained Least Squares (NNLS) described in Supporting Information [25]. The polydispersity index (PDI) is the ratio between the variance of the distribution and the square of the mean value of the decay rate. Then $\bar{\Gamma}$ obtained from the autocorrelation function at angles between 20° and 150° is plotted as a function of q^2 in order to obtain the mean diffusion coefficient and, from Stokes-Einstein equation, the mean hydrodynamic radius according to equation $\bar{\Gamma}=Dq^2$

2.8 Small Angle Neutron Scattering

Small angle neutron scattering measurements were carried out at the KWS-1 diffractometer [26] located at the Maier-Leibnitz Zentrum, Garching, Germany. Neutrons with an average

wavelength of $\lambda = 5.0$ Å and wavelength spread $\Delta\lambda/\lambda \leq 0.10$ were used. A two-dimensional 128 × 128 pixel-based array scintillation detector set at three different collimation (C)/sample-to-detector (D) distances (namely $C_{20}D_2$, $C_{20}D_8$, and $C_{20}D_{20}$, with all distances in meters) measured neutrons scattered from the samples. These configurations allowed collection of data in a range of the scattering vector modulus $Q = 4\pi/\lambda \cdot \sin(\theta/2)$ between 0.00201 and 0.439 $Å^{-1}$, θ being the scattering angle. The investigated samples were contained in a closed quartz cell, in order to prevent the solvent evaporation, and were kept under measurements for a period such as to have at least 2 million counts of neutrons. Temperature was controlled by means of a Peltier-based thermostat, within a range of ± 0.05 °C. The obtained raw data were corrected for background and empty cell scattering, and then radially averaged. Detector efficiency corrections and transformation to absolute scattering cross sections were executed with a secondary Plexiglas standard [27]. Obtained data have been analysed through the software Sasview, using suitable theoretical models: unilamellar vesicles; multilamellar vesicles; homogeneous cylinders, or a combination of them, where appropriate.

2.9 Transmission Electron Microscopy

TEM experiments were performed with a Hitachi HT7700 (Hitachi High Tech, Hitachinaka, Japon) microscope (accelerating voltage of 75 kV). A small drop of aqueous vesicle solution was deposited onto a discharged copper grid coated with a carbon membrane, left few minutes and gently dried with absorbing paper. A drop of uranyl acetate solution was deposited onto the grid for 10 seconds, and the grid was then dried under a lamp for at least 5 minutes. Images were then analysed with ImageJ.

3. RESULTS AND DISCUSSION

3.1. Micron-sized copolymer-lipid hybrid assemblies

Figure 1 presents the structures of the components for the copolymer-lipid hybrid assemblies. The self-assembly behavior in water of both copolymers and lipids is dependent on their structural characteristics, namely, on the relative steric hindrance of the hydrophobic moiety with respect to the hydrophilic one. For lipids, this is described by the packing parameter [28] p ($p = v/a_0 l$), which compares the volume (v) and length (l) of the hydrophobic moiety with the equilibrium surface area of the hydrophilic part (a_0) to predict the shape of self-assemblies, yielding spherical micelles for low values of p (p<1) and then, upon increasing p, elongated micelles, planar structures (p=1) and inverse assemblies (p>1). For copolymers, a qualitative similar trend is found in self-assemblies in water, as a function of the asymmetry between the hydrophilic and the hydrophobic units. Disher and Eisenberg proposed to use the hydrophilic ratio, $f_{\text{hydrophilic}}$, defined as the ratio between the mass of the hydrophilic block and the total mass, as a measure of block copolymer asymmetry influencing the preferred self-assembly geometry. For our systems, DPPC is characterized by a packing parameter p close to 1, while the value of $f_{\text{hydrophilic}}$ of PBD(2300)PEO(900) is roughly 28% in the range where vesicular assemblies are expected for PBD based block copolymers [1,29].

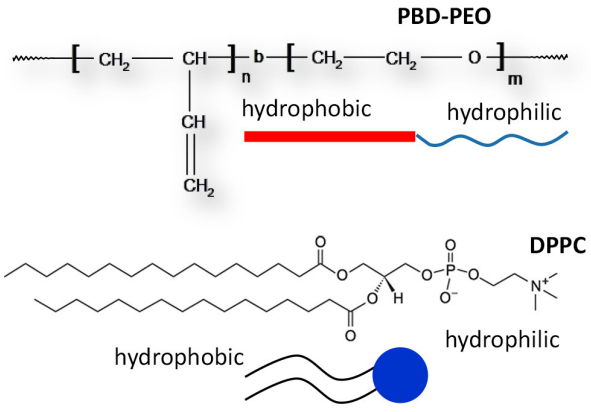

Figure 1. Structure of hybrid vesicles components. Structure of PBD(2300)PEO(900) (polybutadiene (Mw 2300)-b-ethyleneoxide (Mw 900)) copolymer and DPPC (dipalmitoylphosphatidylcholine) lipid. Both building blocks have structural features (steric hindrance balance between the hydrophobic and the hydrophilic moieties) consistent with the self-assembly into vesicular structures.

First, GUVs were formed from different PBD-PEO/DPPC mixtures according to the well-established electroformation method [21,30,31] performed as described in the experimental section. In Figure 2 the morphology of the obtained micro-objects is summarized by representative optical microscopy images. Concerning pure PBD-PEO, it hardly formed vesicles of size higher than 5 μm and difficult to detach from the film (see Figure 2a). This experimental finding is common to other neutral PBD based block copolymers with different molecular weights. Even if we cannot readily demonstrate it, it is possible to hypothesize that the low polarity of the PBD-PEO limits the penetration of water in the dry film and the full hydration and detachment of copolymer layers. As a matter of fact, the addition of a low amount (20 mol %) of the same copolymer carrying a carboxylic acid unit and of similar molecular weight promotes the formation and detachment of the vesicles from the film, possibly thanks to an increased repulsive contribution between the polymer units (see SI Figure S1). DPPC GUVs were polydisperse in size, ranging roughly from 10 μm to 25 μm (see SI Table S1) that easily detached from the lipid film (Figure 2i). Even a small amount (9 mol %) of DPPC added to PBD-PEO strongly promoted the formation of GUVs (Figure 2b) and the presence of GUVs was observed over the whole investigated range of PBD-PEO/DPPC mole ratios. One could argue that phase separation between the copolymer and the lipid might occur and that the GUVs characterized by a higher diameter might be made of pure DPPC. However, it can be observed that the GUVs originating from PBD-PEO/DPPC mixtures are clearly of irregular, not perfectly rounded shape and that regions of slightly different contrasts within the GUVs membranes can be recognized (see Figure

2b-h, insets). Both these effects are evidence of the presence of the two components, lipid and copolymer, in the GUVs. In particular, this ragged surface is reminiscent of the ''bulging out'' domains observed by Nam et al. for other PBD-PEO copolymers mixed with DPPC [32] and has been attributed to the formation of GUVs formed by PIB-PEO in the presence of DPPC [13]. In fact, the slight contrast variation within the membrane could be related to the slight different refractive index of PBD-PEO-rich and DPPC-rich regions. Besides, the membrane thicknesses of the copolymer-based vesicles are generally two to three times higher than those of lipid-based ones [6]. The packing behavior of lipid molecules is probably affected by the presence of the copolymer, in particular at the phase borders, which might give rise to the shape irregularities highlighted in the optical microscopy images.

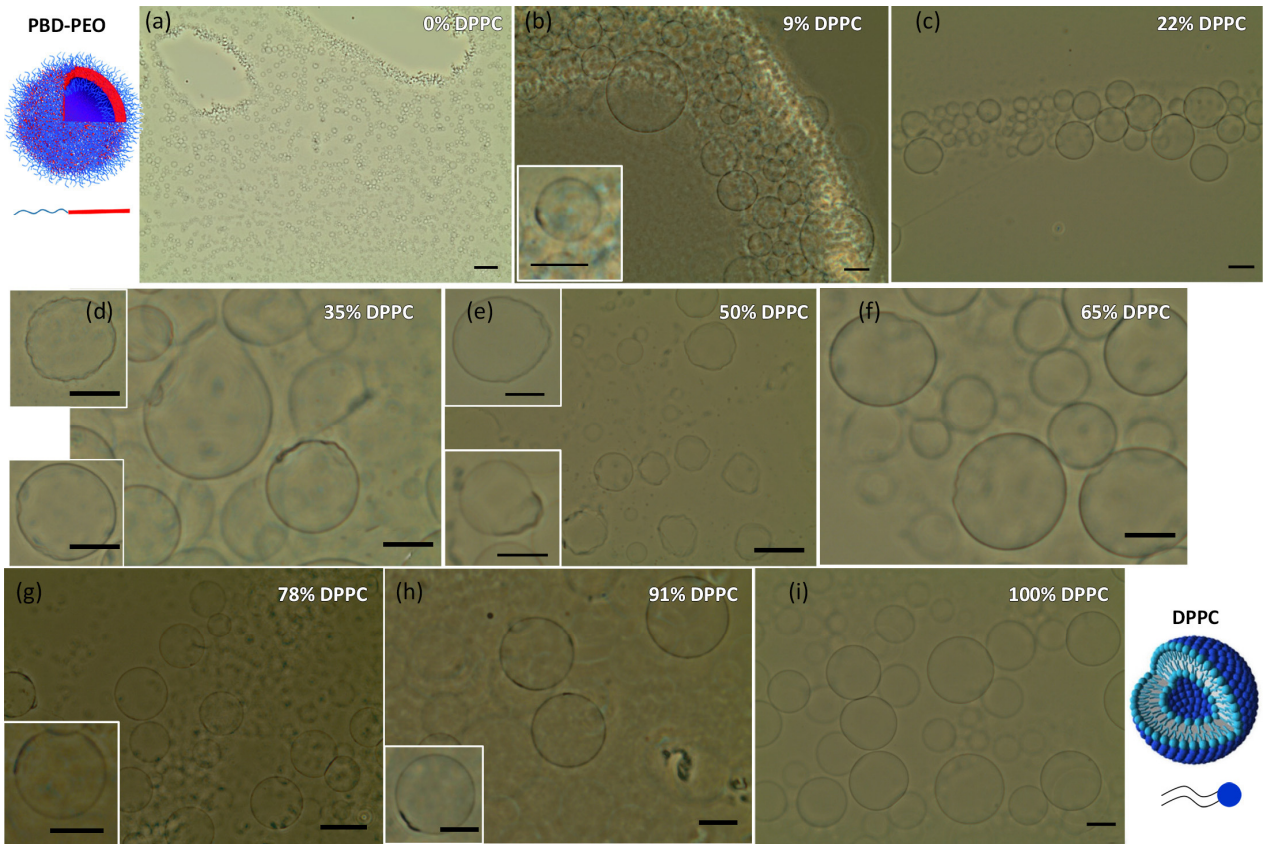

Figure 2. Phase diagram of PEO-PBD/DPPC hybrid GUVs: optical microscopy. Representative optical microscopy images of: (a) PBD-PEO and (i) DPPC pure GUVs; (b-i)

PEO-PBD/DPPC mixed GUVs with increasing DPPC mole percentage, (b) 9%, (c) 22%, (d) 35%, (e) 50%, (f) 65%, (g) 78%, (h) 91%; scale bar 20 µm.

In order to get further insight into the nature of the formed vesicles and to highlight the partition of the two different components, lipid and copolymer, within the GUVs, we performed a confocal microscopy investigation. Two different lipid fluorescent probes were selected, Bodipy (excitation 488 nm, emission 498-530 nm, green) and DiIC20 (excitation 561 nm, emission 571-650 nm, red) with preferential partition for the fluid and the gel phases, respectively. The rigidity of the copolymer is related to its glass transition temperature, which, for PBD-PEO, is well below room temperature; thus, in our experimental conditions the copolymer phase is relatively fluid and preferentially hosts Bodipy molecules. Conversely, as already pointed out, the melting temperature of pure DPPC is around 41°C. Thus, in our experimental conditions pure DPPC assemblies are arranged in L_β phase with the saturated hydrophobic chains orderly packed, resulting in a rigid structure, which preferentially hosts DiIC20 molecules. Figure 3 shows representative confocal microscopy images of GUVs made of pure copolymer (Figure 3a-c) and pure lipid (Figure 3d-f), respectively, containing both Bodipy and DiIC20 dyes embedded in the membrane. Both GUVs made of pure copolymer and of pure DPPC are characterized by a homogeneous distribution of the two fluorescent dyes within the membrane, as expected for a monophasic system where no partition occurs.

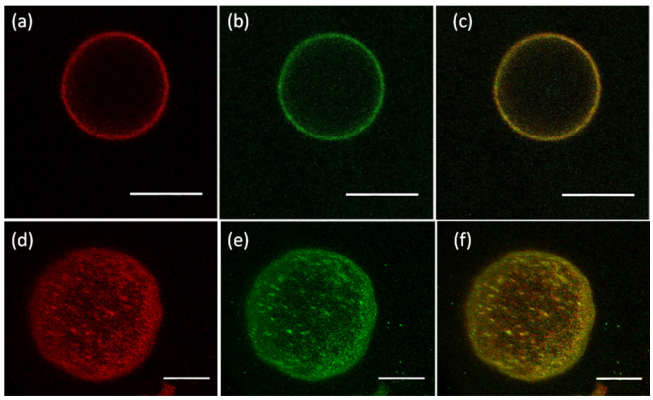

Figure 3. PEO-PBD and DPPC pure GUVs: confocal microscopy. Representative CLSM images of (a-c) PBD-PEO vesicles (PBD-PEO mixed with 20% mol/mol PBD-PEO-COOH) (2D) and (d-f) DPPC vesicles (3D reconstructions); (a, d) first channel with DiIC20 fluorescence (red, excitation 561 nm, emission 571-650 nm), (b, e) second channel with Bodipy fluorescence (green, excitation 488 nm, emission 498-530 nm), (c, e) overlay of the first and second channel (yellow). Scale bar 10 μm.

In Figure 4, representative confocal microscopy images are displayed for PBD-PEO/DPPC hybrid GUVs containing 35 mol % DPPC (Figure 4a-b) and 65 mol % DPPC (Figure 4c-e), respectively. In these samples, a clear inhomogeneous distribution of the two dyes is observed, with micron-sized domains where DiIC20 fluorescence (red) is concentrated, clearly separated from Bodipy fluorescence (green). Small copolymer-rich domains always form in a lipid-rich GUV independently of the blend composition. As the polymer alone difficultly forms GUVs, it is probably prone to insert in GUVs mainly constituted by DPPC. This kind of hybrid GUVs, characterized by phase separated domains, has already been reported on copolymer/DPPC systems [13,32] and for hydrophobic mismatches as high as those of the investigated systems, they are spherical. Besides, it has been observed that size of the domains is influenced by the cooling rate after electroformation because DPPC undergoes a phase transition from a liquid-like phase to a gel phase. High cooling rate induces the formation of small round domains in a similar way as a nucleation phenomenon. As we did not control the cooling rate we cannot comment on the domains size distribution. Nevertheless, we can observe that the overall GUV surface covered by domains is not homogeneously distributed within different GUVs, probably indicating that the composition of each GUV does not necessarily correspond to the initial one in the blend. Given that GUVs are not thermodynamically stable assemblies, it can be hypothesized that the amount of phase segregated copolymer-rich fluid phase (where Bodipy is concentrated), with respect to lipid-rich rigid phase (where DiIC20 preferentially partition), is connected to the variability in the composition of the film from which the GUVs are

electroformed. Nevertheless, confocal microscopy data fully confirm optical microscopy data, highlighting that PBD-PEO and DPPC can be mixed in a broad range of molar ratios to form hybrid micron-sized vesicular assemblies.

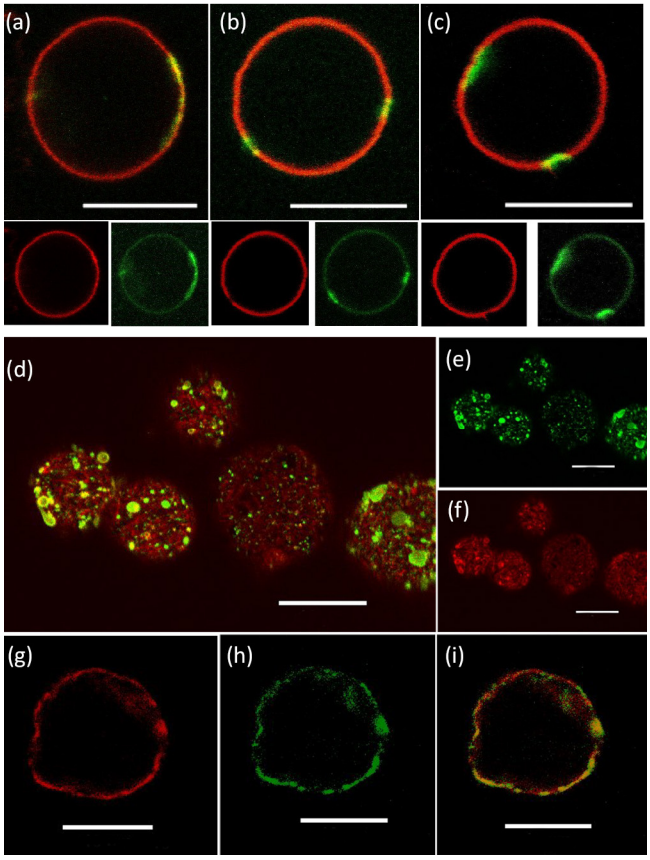

Figure 4. PEO-PBD/DPPC mixed GUVs: confocal microscopy. Representative CLSM images of PEO-PBD/DPPC mixed vesicles containing (a-c) 35% and (d-i) 65% DPPC with respect to PEO-PBD (mol%). For each image DiIC20 fluorescence (red, excitation 561 nm, emission 571-650 nm), (b, e) and Bodipy fluorescence (green, excitation 488 nm, emission 498-530 nm) are both displayed as separate channels and as overlay (yellow). Scale bar 10 μm.

In order to better investigate the properties of the obtained hybrid systems, a home-built microfluidic set-up was employed to get insights on the viscoelastic properties of the hybrid GUVs with respect to the purely lipid-composed or copolymer-composed vesicles.

Figure 5a presents the microfluidic set-up: briefly, constrictions (U-shaped traps, opening width 10 to 20 µm) placed along linear microfluidic channels blocked individual GUVs larger than trap width, injected in the channel. The traps were used to probe the mechanics of each GUV: the way an increase of the flow (controlled here by the pressure difference between inlet and outlet) affected GUV shape determined a qualitative relationship between mechanical stress and vesicle deformation. The mechanical stress is a combination of (i) the pressure difference upstream/downstream the trap and (ii) the drag force due to remaining fluid flow around the object. A quantitative description is out of the scope of the present paper and will be described in a future work.

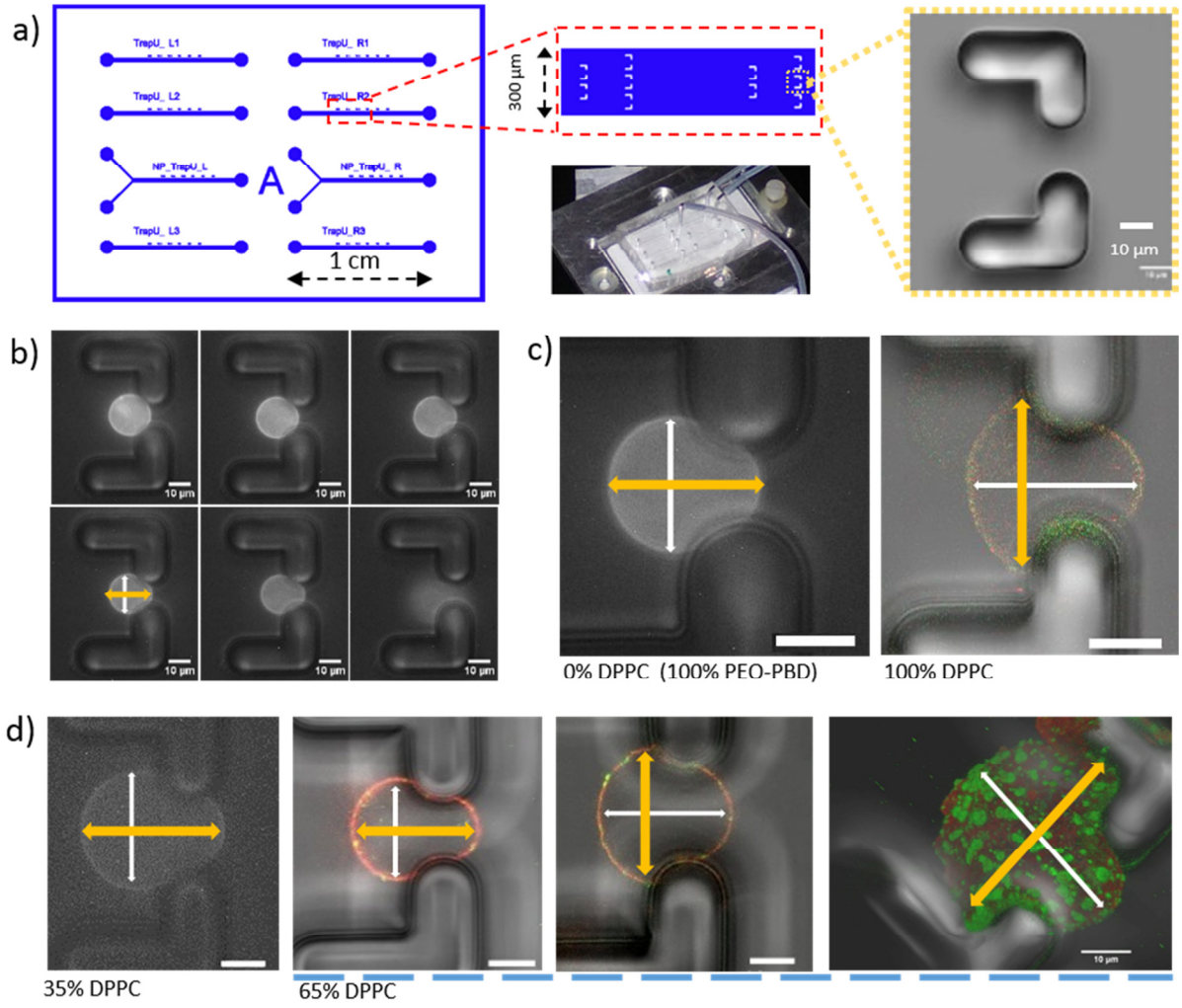

Figure 5. PEO-PBD/DPPC mixed GUVs: microfluidics. a) Representative microfluidic set-up: design showing several single channels on a 24x32mm chip, close-up of the channel zone including U-shape traps, microphotograph of a single trap with 14 µm opening. b) Progressive deformation of a vesicle with pure PEO-PBD composition, upon pressure increase from 1 mBar (top left) to 31 mBar (bottom right) at which the vesicle escapes. c) Deformation modes observed with pure polymer vesicles (longitudinal, along the flow) and pure lipid vesicles (transverse, perpendicular to the flow). d) Deformation modes observed with hybrid GUV: all GUV containing 35 mol % DPPC deform along the flow, whereas for 65 mol % DPPC, different behaviors are observed. Scale bar 10 µm.

In Figure 5b, the typical progressive deformation for pure polymer GUV is shown, with pressure difference (inlet to outlet) increasing from 1 mBar to 31 mBar at which point the GUV escapes the trap (flow is from left to right). As visualized by the thick yellow arrow, this vesicle deforms

in the longitudinal (flow) direction, whereas its dimension in the transverse direction (white thin arrow) is almost unchanged. This behavior is observed for all GUVs with pure polymeric composition, as shown in left panel of Figure 5c (100% PEO-PBD, equivalent to 0% DPPC), which we interpret as a quite fluid-like behavior of the polymeric GUV membrane, which starts "flowing" within the trap. This is consistent with the fact that the polymer is well above its glass transition temperature, leading to mobile chains within the polymersome. On the contrary, pure lipid DPPC GUVs deform in a transverse way while the flow intensity is increased (Figure 5c, right panel), more in an "elastic-like" behavior, the GUV being flattened out on the trap. We attribute such a deformation mode resembling that of a solid to the fact that DPPC is in the gel phase at room temperature. For hybrid vesicles, shown in Figure 5d, we observe two main features. First, GUVs mainly composed of polymer (35 mol % DPPC) all experience a longitudinal, liquid-like, deformation: this is an indication that their properties are governed by the polymers, in spite of domain formation. Second, hybrid objects at 65 mol % DPPC show much more variability from one GUV to the other: some show longitudinal deformation like pure polymer, whereas others are more comparable to transverse flattening typical of DPPC GUVs. This could be due to a variability in GUV composition, which is plausible since each object originates from a different zone of the film, consistently with the CLSM observations. Note however that we observe micron-sized domains in trapped objects for both types of behaviors (see for example the last image in Figure 5d).

3.2. Nano-sized copolymer-lipid hybrid assemblies

As already discussed, one of the main applications of lipid-based and copolymer-based assemblies is the development of drug delivery systems for Nanomedicine. In this respect, hybrid systems have been receiving a lot of attention recently, due to the inherent possibilities they offer

to combine and modulate the characteristics of lipid-based and copolymer-based assemblies in order to strongly enhance their performances.

Hybrid PBD-PEO/DPPC nano-objects were prepared through dry film rehydration and extrusion through a 100 nm polycarbonate membrane, according to a well-established procedure for the formation of nanometric liposomes, [33] as described in the experimental section. The as-prepared dispersions were characterized through multiangle dynamic light scattering. In Figure 6a, representative DLS curves of the pure PBD-PEO and DPPC vesicles' dispersion are displayed together with those obtained for PBD-PEO/DPPC hybrid systems (with 35 mol % and 65 mol % DPPC, respectively) acquired at 150°. From the comparison of the autocorrelation functions of the scattered intensity (ACF) profiles, it is apparent that hybrid systems are characterized by lower decay times with respect to the pure assemblies. The mean hydrodynamic radius and polydispersity of the nano-objects were obtained with the NNLS analysis of the ACF and are reported in Table 1. As anticipated from the observation of DLS curves, the hydrodynamic radii of hybrid self-assembled objects are lower than those obtained from the pure objects. Moreover, their size is lower than the polycarbonate membrane pores employed for extrusion.

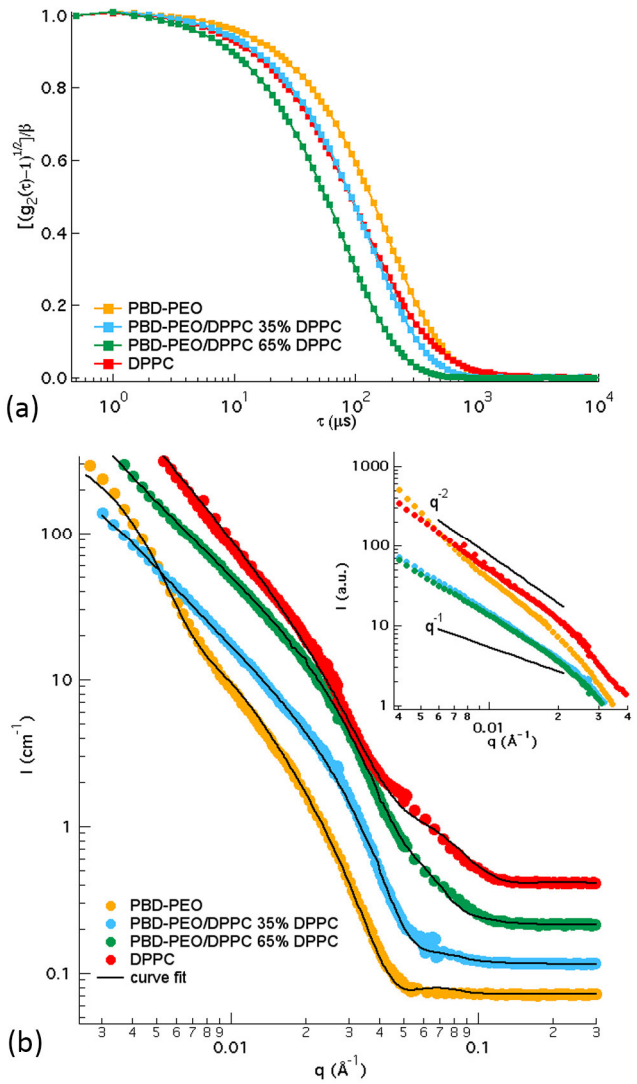

Figure 6. PEO-PBD/DPPC mixed LUV: DLS and SANS. (a) Representative normalized DLS curves of PBD-PEO (yellow markers), PBD-PEO/DPPC 35 mol % (blue markers), PBD-PEO/DPPC 65 mol % (green markers), DPPC (red markers) nano-assemblies dispersions, acquired at 150°; (b) representative SANS curves of PBD-PEO (yellow markers), PBD-PEO/DPPC 35 mol % (blue markers), PBD-PEO/DPPC 65 mol % (green markers), DPPC (red markers) nano-assemblies dispersions in D_2O and curve fitting (continuous black lines) of the experimental curves, according to a combined vesicle and cylinder form factor model; (b, inset) intermediate q-range of the same curves: the curves are displayed with a suitable offset and $I = q^{-2}$ and $I = q^{-1}$ trends are displayed, to facilitate the slope analysis of the curves.

In order to obtain more detailed information on the shape of hybrid nano-objects, the same samples prepared in D_2O were analyzed through Small-Angle Neutron Scattering (SANS). In Figure 6b the SANS profiles obtained for the different systems are compared, while in the inset

the intermediate *q*-range is displayed. Interestingly, a different slope is observed for the different systems at intermediate q range: in particular, PBD-PEO and DPPC pure nano-objects are characterized by a q^{-2} trend (see Figure 6b, inset), which is typical for 2D assemblies, as vesicles; the trend of both DPPC 35 mol % and DPPC 65 mol % PBD-PEO/DPPC hybrids is in-between a q^{-1} and a q^{-2} slope, which suggests the coexistence of vesicular and cylindrical nano-assemblies. SANS curves were analyzed according to a combined form factor of vesicles and cylinders with a Schultz distribution in size and thickness. The resulting fitting curves are shown in Figure 6b, while the fitting results are reported in Table 1. Consistently with the slope analysis of the SANS curves in the intermediate q region, the hybrid systems can be described by a mixture of cylindrical and vesicular objects, whose percentages (reported in Table 1 as v%, vesicles percentage) can be roughly evaluated as the relative volume fraction of the two types of assemblies, as obtained from the fitting procedure. With respect to the membrane thickness, a linear change (from around 12 nm for the pure copolymer vesicles to around 4 nm for pure lipid vesicles, see Table 1, Th_v values) is observed, which can be a first evidence of the formation of hybrid objects at the nanoscale. Interestingly, the cylindrical assemblies are characterized by a defined radius (around 7.5 nm, see R_c values in Table 1) and a very low polydispersity (see PDI (R_c) values in Table 1), irrespectively to the lipid amount.

	DLS		SANS				
composition	R_h (nm)	PDI	v%	Th_v (nm)	PDI (Th_v)	R_c (nm)	PDI (R_c)
PBD-PEO	68	0.32	100	12.2	0.2	-	-
PBD-PEO/DPPC 35%	46	0.39	47.7	7.27	0.2	7.7	0.01
PBD-PEO/DPPC 65%	30	0.46	67.3	4.94	0.4	7.5	0.05
DPPC	55	0.41	100	3.9	0.2	-	-

Table 1. PEO-PBD/DPPC mixed LUV: DLS and SANS fitting results. (DLS) Hydrodynamic radius (Rh) and polydispersity index (PDI) obtained from the analysis of the autocorrelation functions of the scattered intensity for the colloidal dispersions of the different nano-objects; (SANS) fitting results obtained from the analysis of SANS curves according to a combined vesicles-cylinders form factor: relative percentage of vesicles with respect to cylinders (v%); membrane thickness (Th_v) and membrane thickness polydispersity (PDI (Th_v)) of vesicles; radius of cylinders (R_c) and polydispersity of the radius of cylinders (PDI (R_c)).

The SANS results are confirmed by the TEM micrographs of the different systems displayed in Figure 7. In Figure 7a and 7b vesicles of pure PBD-PEO and pure DPPC, respectively, are visualized. Consistently with SANS results, only vesicles of slightly polydisperse sizes are present. In Figure 7c-f representative TEM micrographs of PBD-PEO/DPPC hybrids are displayed. Amazingly, in this case a high amount of cylindrical micelles is present coexisting with fewer vesicles. Interestingly in the 35 mol % sample, typical intermediate structures (inset in Figure 7c), signature of the transition from vesicles to worm-like micelles, are observed. This kind of intermediate structure has been observed in the worm to vesicle transition during polymerization induced self-assembly which can be attributed to a decrease in the hydrophilic ratio during polymerization [34]. As already discussed, cylindrical micelles are completely absent in both samples of pure copolymer and pure DPPC, as highlighted both by SANS and TEM data. Thus, these wormlike nanoassemblies are clearly hybrid assemblies. Very recently the presence of worm-like micelles has also been observed in hybrid systems based on triblock PEO_{17}-$PDMS_{67}$-PEO_{17} mixed with DPPC [5] and on PBD_{22}-PEO_{14} mixed with POPC [3]. For PDMS based systems, this transition is observed only for high hydrophobic mismatch. Our results nicely confirm these reports, bringing to the conclusion that morphological transitions are directly related to intimate lipid/polymer mixing.

From the micron-scale investigation it has been highlighted that PBD-PEO/DPPC GUVs can form hybrid vesicular assemblies with micron-sized domains of copolymer rich and lipid rich

phases coexisting within the same GUV. These domains are clearly relevant features of the hybrid GUVs' membrane, determining irregularly shaped regions and tunable viscoelastic properties. However, this micron-sized phase segregation is not possible in nano-objects. In the self-assembly of copolymer-lipid hybrids into wormlike assemblies we can thus hypothesize that, due to the small size of the objects, phase segregation is energetically disfavored due to the strong difference in their spontaneous curvature and copolymer and lipid mix at a molecular level, to form cylindrical assemblies of high curvature.

The different protocols employed for the preparation of the objects at the micro- and nano-scale may play a role. We can’t exclude that the differently shaped objects at the two length-scales would result from the interplay between thermodynamic stabilization and kinetic control, which is different according to the preparation protocol.

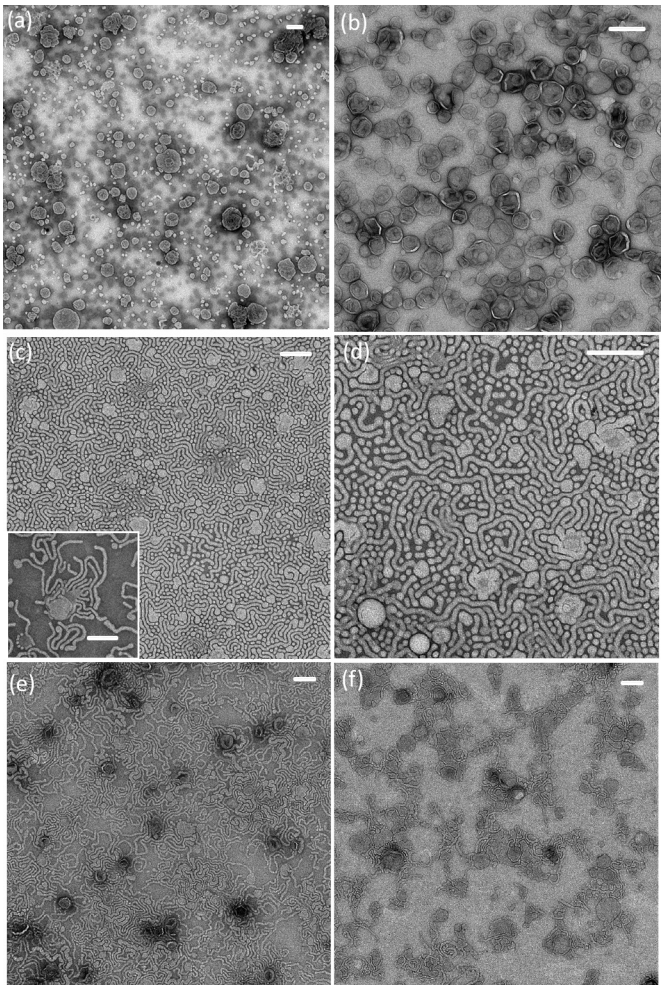

Figure 7. PEO-PBD/DPPC mixed LUV: TEM. Representative TEM micrographs of: (a)PBD-PEO and (b) DPPC nanometric vesicles; (c-f) PBD-PEO/DPPC hybrid nanometric assemblies containing (c, d) 35% DPPC and (e, f) 65% DPPC molar ratios. Scale bars of 200 nm.

CONCLUSION

In this study we have explored the main physicochemical, structural and mechanical features of lipid-copolymer hybrid assemblies composed of dipalmitoylphosphatidylcholine (DPPC) and polybutadiene-co-polyethyleneoxide (PBD-PEO) both at the micro and at the nano lengthscales. Concerning the microscale, optical microscopy images highlight that hybrid Giant Unilamellar Vesicles (GUVs) are efficiently formed in a broad range of PBD-PEO/DPPC molar ratios.

Hybrid GUVs are characterized by irregular shapes and compositional inhomogeneities. The occurrence of lateral phase separation in lipid-rich and copolymer-rich regions was proved through Confocal Microscopy experiments, which highlighted the coexistence of areas of higher fluidity enriched with the copolymer, whose Tg is well below room temperature, with areas of lower fluidity, with higher amounts of DPPC, which is below its gel-to-liquid crystalline transition temperature. The presence and distribution of these phase-separated domains deeply affect the mechanical and viscoelastic properties of the hybrid GUVs, as proved through microfluidic trapping. Concerning the nano lengthscale, both pure DPPC and pure PBD-PEO self assemble into nanosized vesicles; conversely, copolymer-lipid hybrids preferentially self-assemble into elongated, worm-like objects with highly monodisperse cross-section. This evidence, confirmed both by SANS and TEM results, clearly proves that the composition of these worm-like objects is hybrid. We hypothesize that the lateral micron-sized phase separation, which is observed for GUVs, is energetically disfavored when the lengthscale of the self-assembled objects decreases, due to the large hydrophobic mismatch between the lipid and the copolymer. Thus, at the nanoscale, instead of small unilamellar vesicles with nanosized domains or fully demixed separated vesicles of pure DPPC and pure PBD-PEO, cylindrical micelles are formed. The self-assembly pathway and the arrangement of the two components is completely changed with respect to the micron-lengthscale. Overall, we show that the preparation methodology, the lengthscale of the objects, the initial composition of copolymer-lipid blend can be varied to modulate the morphology, size, shape and mechanical properties of these versatile hybrid self-assemblies.

ACKNOWLEDGMENTS

This work has been carried out in the framework of the ANR Polytransflow (13-BS09-0015). This work was partly supported by LAAS-CNRS micro and nanotechnologies platform member of the French RENATECH network. We acknowledge funding from CNRS PICS program "Microfluidics for Soft Matter", Jülich Centre for Neutron Science and Maier-Leibnitz Zentrum are fully acknowledged for provision of beam time. Technische Universität München is acknowledged for support of travel expenses. CM acknowledges ANR Poytransflow (13-BS09-0015) for funding; BL and PJ would like to thank Prof. Piero Baglioni for the scientifically stimulating stay at CSGI- Florence; CM and DB are grateful to CSGI for financial support and to Prof. Piero Baglioni for fruitful discussions.

ASSOCIATED CONTENT

Supplementary Optical Microscopy images, GUVs' size analysis and DLS stability data are reported as supporting information.

REFERENCES

[1] D.E. Discher, A. Eisenberg, Polymer vesicles, Science. 297 (2002) 967–974. doi:10.1126/science.1074972.

[2] Y. Zhu, B. Yang, S. Chen, J. Du, Polymer vesicles: Mechanism, preparation, application, and responsive behavior, Prog. Polym. Sci. 64 (2017) 1–22. doi:10.1016/j.progpolymsci.2015.05.001.

[3] M. Schulz, W.H. Binder, Mixed hybrid lipid/polymer vesicles as a novel membrane platform, Macromol. Rapid Commun. 36 (2015) 2031–2041. doi:10.1002/marc.201500344.

[4] T.P.T. Dao, F. Fernandes, M. Er-Rafik, R. Salva, M. Schmutz, A. Brulet, et al., Phase separation and nanodomain formation in hybrid polymer/lipid vesicles, ACS Macro Lett.

4 (2015) 182–186. doi:10.1021/mz500748f.

[5] T.P.T. Dao, A. Brûlet, F. Fernandes, M. Er-Rafik, K. Ferji, R. Schweins, et al., Mixing Block Copolymers with Phospholipids at the Nanoscale: From Hybrid Polymer/Lipid Wormlike Micelles to Vesicles Presenting Lipid Nanodomains, Langmuir. 33 (2017) 1705–1715. doi:10.1021/acs.langmuir.6b04478.

[6] T. Ruysschaert, A.F.P. Sonnen, T. Haefele, W. Meier, M. Winterhalter, D. Fournier, Hybrid nanocapsules: Interactions of ABA block copolymers with liposomes, J. Am. Chem. Soc. 127 (2005) 6242–6247. doi:10.1021/ja043600x.

[7] W. Shen, J. Hu, X. Hu, Impact of amphiphilic triblock copolymers on stability and permeability of phospholipid/polymer hybrid vesicles, Chem. Phys. Lett. 600 (2014) 56–61. doi:10.1016/j.cplett.2014.03.057.

[8] S.K. Lim, H.P. de Hoog, A.N. Parikh, M. Nallani, B. Liedberg, Hybrid, nanoscale phospholipid/block copolymer vesicles, Polymers (Basel). 5 (2013) 1102–1114. doi:10.3390/polym5031102.

[9] S. Khan, M. Li, S.P. Muench, L.J.C. Jeuken, P.A. Beales, Durable proteo-hybrid vesicles for the extended functional lifetime of membrane proteins in bionanotechnology, Chem. Commun. 52 (2016) 11020–11023. doi:10.1039/C6CC04207D.

[10] Z. Cheng, D.R. Elias, N.P. Kamat, E.D. Johnston, A. Poloukhtine, V. Popik, et al., Improved tumor targeting of polymer-based nanovesicles using polymer-lipid blends, Bioconjug. Chem. 22 (2011) 2021–2029. doi:10.1021/bc200214g.

[11] T.P.T. Dao, F. Fernandes, E. Ibarboure, K. Ferji, M. Prieto, O. Sandre, et al., Modulation of phase separation at the micron scale and nanoscale in giant polymer/lipid hybrid unilamellar vesicles (GHUVs), Soft Matter. 13 (2017) 627–637.

doi:10.1039/C6SM01625A.

[12] J. Nam, P.A. Beales, T.K. Vanderlick, Giant phospholipid/block copolymer hybrid vesicles: Mixing behavior and domain formation, Langmuir. 27 (2011) 1–6. doi:10.1021/la103428g.

[13] M. Schulz, D. Glatte, A. Meister, P. Scholtysek, A. Kerth, A. Blume, et al., Hybrid lipid/polymer giant unilamellar vesicles: effects of incorporated biocompatible PIB–PEO block copolymers on vesicle properties, Soft Matter. 7 (2011) 8100. doi:10.1039/c1sm05725a.

[14] R.P. Brinkhuis, F.P.J.T. Rutjes, J.C.M. van Hest, Polymeric vesicles in biomedical applications, Polym. Chem. 2 (2011) 1449. doi:10.1039/c1py00061f.

[15] J.P. Jain, W.Y. Ayen, N. Kumar, Self assembling polymers as polymersomes for drug delivery., Curr. Pharm. Des. 17 (2011) 65–79. doi:10.2174/138161211795049822.

[16] L. Simeone, G. Mangiapia, C. Irace, A. Di Pascale, A. Colonna, O. Ortona, et al., Nucleolipid nanovectors as molecular carriers for potential applications in drug delivery, Mol. Biosyst. 7 (2011) 3075–3086. doi:10.1039/c1mb05143a.

[17] A.L. Klibanov, K. Maruyama, V.P. Torchilin, L. Huang, Amphipathic polyethyleneglycols effectively prolong the circulation time of liposomes, FEBS Lett. 268 (1990) 235–237. doi:10.1016/0014-5793(90)81016-H.

[18] X. Su, S.K. Mohamed Moinuddeen, L. Mori, M. Nallani, Hybrid polymersomes: facile manipulation of vesicular surfaces for enhancing cellular interaction, J. Mater. Chem. B. 1 (2013) 5751. doi:10.1039/c3tb21111h.

[19] K. Pressl, K. Jorgensen, P. Laggner, Characterization of the sub-main-transition in distearoylphosphatidylcholine studied by simultaneous small- and wide-angle X-ray

diffraction, Biochim. Biophys. Acta - Biomembr. 1325 (1997) 1–7. doi:10.1016/S0005-2736(97)00013-8.

[20] A. Salvatore, C. Montis, D. Berti, P. Baglioni, Multifunctional Magnetoliposomes for Sequential Controlled Release, ACS Nano. 10 (2016) 7749–7760. doi:10.1021/acsnano.6b03194.

[21] M.I. Angelova, S. Soléau, P. Méléard, F. Faucon, P. Bothorel, Preparation of giant vesicles by external AC electric fields. Kinetics and applications, in: C. Helm, M. Lösche, H. Möhwald (Eds.), Trends Colloid Interface Sci. VI SE - 29, Steinkopff, 1992: pp. 127–131. doi:10.1007/BFb0116295.

[22] D.C. Duffy, J.C. McDonald, O.J.A. Schueller, G.M. Whitesides, Rapid prototyping of microfluidic systems in poly(dimethylsiloxane), Anal. Chem. 70 (1998) 4974–4984. doi:10.1021/ac980656z.

[23] R. Courson, S. Cargou, V. Conedera, M. Fouet, M.C. Blatche, C.L. Serpentini, et al., Low-cost multilevel microchannel lab on chip: DF-1000 series dry film photoresist as a promising enabler, RSC Adv. 4 (2014) 54847–54853. doi:10.1039/C4RA09097G.

[24] U. Till, M. Gaucher, B. Amouroux, S. Gineste, B. Lonetti, J.D. Marty, et al., Frit inlet field-flow fractionation techniques for the characterization of polyion complex self-assemblies, J. Chromatogr. A. 1481 (2017) 101–110. doi:10.1016/j.chroma.2016.12.050.

[25] B.J. Frisken, Revisiting the Method of Cumulants for the Analysis of Dynamic Light-Scattering Data, Appl. Opt. 40 (2001) 4087. doi:10.1364/AO.40.004087.

[26] H. Frielinghaus, A. Feoktystov, I. Berts, G. Mangiapia, KWS-1□: Small-angle scattering diffractometer, J. Large-Scale Res. Facil. 1 (2015) 1–4. doi:http://dx.doi.org/10.17815/jlsrf-1-26.

[27] G.D. Wignall, F.S. Bates, Absolute Calibration of Small-Angle Neutron Scattering Data *, J. Appl. Crystallogr. 20 (1987) 28–40. doi:10.1107/S0021889887087181.

[28] J.N. Israelachvili, S. Marcelja, R.G. Horn, Physical principles of membrane organization., Q. Rev. Biophys. 13 (1980) 121–200. doi:10.1017/S0033583500001645.

[29] S. Hocine, M.-H. Li, Thermoresponsive self-assembled polymer colloids in water, Soft Matter. 9 (2013) 5839. doi:10.1039/c3sm50428j.

[30] S. Smeazzetto, F. Tadini-Buoninsegni, G. Thiel, D. Berti, C. Montis, Phospholamban spontaneously reconstitutes into giant unilamellar vesicles where it generates a cation selective channel, Phys. Chem. Chem. Phys. (2016). doi:10.1039/C5CP05893G.

[31] C. Montis, S. Sostegni, S. Milani, P. Baglioni, D. Berti, Biocompatible Cationic Lipids for the Formulation of Liposomal DNA Vectors, Soft Matter. 10 (2014) 4287–97. doi:10.1039/c4sm00142g.

[32] J. Nam, T.K. Vanderlick, P.A. Beales, Formation and dissolution of phospholipid domains with varying textures in hybrid lipo-polymersomes, Soft Matter. 8 (2012) 7982. doi:10.1039/c2sm25646k.

[33] A. Marín-Menéndez, C. Montis, T. Díaz-Calvo, D. Carta, K. Hatzixanthis, C.J. Morris, et al., Antimicrobial Nanoplexes meet Model Bacterial Membranes: the key role of Cardiolipin, Sci. Rep. 7 (2017) 41242. doi:10.1038/srep41242.

[34] A. Blanazs, J. Madsen, G. Battaglia, A.J. Ryan, S.P. Armes, Mechanistic insights for block copolymer morphologies: How do worms form vesicles?, J. Am. Chem. Soc. 133 (2011) 16581–16587. doi:10.1021/ja206301a.